Nanomedicine

ISSN: (Print) (Online) Journal homepage: www.tandfonline.com/journals/innm20

Plasma-Treated Collagen Functionalized With Chondroitin Sulfate as Bioactive and Nanostructured Extracellular Matrix Mimics

Federica Barbugian, Francesca Cadamuro, Francesco Nicotra, Claudia Riccardi & Laura Russo

To cite this article: Federica Barbugian, Francesca Cadamuro, Francesco Nicotra, Claudia Riccardi & Laura Russo (2024) Plasma-Treated Collagen Functionalized With Chondroitin Sulfate as Bioactive and Nanostructured Extracellular Matrix Mimics, Nanomedicine, 19:9, 799-810, DOI: 10.2217/nnm-2023-0310

To link to this article: https://doi.org/10.2217/nnm-2023-0310

Published online: 22 Feb 2024.

Short Communication

For reprint orders, please contact: reprints@futuremedicine.com

Nanomedicine

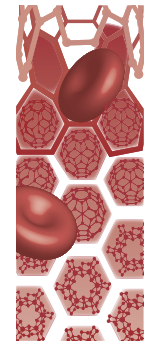

Plasma-treated collagen functionalized with chondroitin sulfate as bioactive and nanostructured extracellular matrix mimics

Federica Barbugian[1], Francesca Cadamuro[1], Francesco Nicotra[1], Claudia Riccardi*,[2] & Laura Russo**,[1]

[1]School of Medicine and Surgery, University of Milano-Bicocca, Vedano al Lambro, 20854, Italy

[2]Department of Physics, University of Milano-Bicocca, Milan, 20126, Italy

*Author for correspondence: claudia.riccardi@unimib.it

**Author for correspondence: laura.russo@unimib.it

Aim: Cell microenvironment contains a plethora of information that influences cell modulation. Indeed, the extracellular matrix plays a central role in tissue development. Reproducing the cell–extracellular matrix crosstalk able to recapitulate both physical and biochemical signals is crucial to obtain functional tissue models or regenerative strategies. **Materials & methods:** Here, a combined method is proposed to easily functionalize collagen surface films, tailoring morphological properties. Oxygen nonthermal plasma treatment and glyco-conjugation with chondroitin sulfate are used to modify surface properties. **Results:** It results in higher adhesion, proliferation and morphological organization of U87 glioblastoma cells. **Conclusion:** Our finding suggests new promising strategies for the development of collagen-based biomaterials, which can be employed for advanced *in vitro* models.

First draft submitted: 26 October 2023; Accepted for publication: 24 January 2024; Published online: 22 February 2024

Keywords: biomaterials • chondroitin sulfate • collagen • ECM mimic • glycans • plasma

The extracellular matrix (ECM) has a driving role in cell fate modulation [1] in healthy and pathological states. Different ECM components and microenvironmental factors are involved in the crosstalk with cells [2]. In glioblastoma, in particular, the contribution of the ECM seems to be critical in the tumor development, progression and resistance to therapies [3]. To decipher the combination of signals provided by the ECMs that determine the cell fate, a large number of synthetic ECMs covering as much as possible the range of their morphological and biochemical properties is needed [4].

Collagens (COLs) [5,6] and glycosaminoglycans (GAGs), which are ubiquitous components of native tissues, are widely employed for the fabrication of scaffolds mimicking natural ECM [7,8]. Indeed, COL is known to play a role in cell adhesion and proliferation [9]. Between sulfated GAGs, chondroitin sulfate (CS) is largely present in the ECM and in the glycocalyx where it plays crucial roles in cell adhesion, signaling, differentiation and migration [10,11]. Importantly, it governs the kinetics of integrin transport and the assembly of integrins into mature adhesion sites [12–15]. Atypical accumulation of CS has been observed in pathological conditions such as glioblastoma [16,17]. Hence, the potential CS-GAGs' interaction with cell motility and adhesion factors suggest the possibility of a plausible mechanism driven by CS-GAG sulfation that contributes to brain tumor invasion.

For this reason, COL and CS are widely used to design materials with potential biomedical applications, especially for tissue regeneration and wound healing [18–22]. The development of hybrid biomaterials composed by COL and CS has been investigated for biomedical applications using both blended and crosslinked scaffolds [23–25]. Recently the same approach has been applied to *in vitro* culture for the generation of biopolymers and tools able to replicate pathological ECMs, such as 3D Glioblastoma Multifome (GBM) models [16,26].

However, the production of ECM mimics is still limited to the development of hybrid systems, where the majority of the efforts are focused on achieving the required morphology while forgetting the role of the biomolecular signals. Therefore, methodologies to finely tune both the physical and biochemical properties of the synthesized

Taylor & Francis
Taylor & Francis Group

ECM mimetic are still needed [16]. In this scenario, one possibility consists in the surface grafting by nonthermal plasma (NTP) modification without affecting materials' bulk properties [27]. NTP in a vacuum generates a few electrical charges, electrons and ions and many different functional groups, depending on the gas precursor employed. The nonthermal equilibrium between species ensures low working temperatures and ion fluxes, avoiding thermal damage of polymeric biodegradable substrates. Surface modification by NTP treatment is a widely used method to enhance the biocompatibility of biomaterials. Plasma treatment is probably one of the most versatile surface treatment techniques at the only cost of owning a vacuum system able to host the reactions [28]. Different types of functionalization can be developed: physical modification (patterned surfaces) [29], chemical modification (functionalized surfaces) [28] and a combination of physical and chemical modifications (superhydrophobic, superhydrophilic surfaces) [30], in order to modulate wettability, surface topography and surface charge to control tissue adhesion, growth and proliferation. Modification by plasma treatment is usually induced by different types of gaseous precursors and is limited to the top surfaces for several hundred angstroms [31]. In particular NTP produced at low pressure with inert and oxygen gas precursors is able to induce morphological modification at the nanoscale providing the unique surface properties required by various applications [32], such as the increase of the surface area by hierarchical ordered nanostructures, and complex fractal interfaces mimicking the surfaces existing in nature [33]. This technique can be efficiently combined with the use of CS in order to benefit from improved adhesion to the substrate material [34] and cell signaling modulation [35].

Here in this work, we propose the development of hybrid surfaces based on COL modified by NTP treatment to introduce 3D nanostructured patterns and covalent conjugation of CS to generate bioactivate surfaces able to actively crosstalk with cells. The proposed approach combines physical and chemical methods to control and modulate the surface properties in order to study their combined effect using U87 glioblastoma cell line.

Materials & methods

Materials

COL from bovine Achilles tendon, acetic acid, sodium cyanoborohydride, 2-(N-morpholino)ethanesulfonic acid buffer (MES) hydrate, U87 glioblastoma cell line, fetal bovine serum, penicillin, streptomycin, phosphate-buffered saline (PBS), bovine serum albumin, sucrose, manganese (II) chloride, paraformaldehyde, DMEM and live/dead assay kit were purchased from Sigma-Aldrich (Milan, Italy). CS was purchased from Carbosynth (Berkshire, UK). Ethanol and citrate buffer pH 6.0 were obtained from Honeywell (Monza, Italy). Alexa Fluor 647 Phalloidin and 4′,6-diamidino-2-phenylindole (DAPI) were from Thermo Fisher Scientific (Monza, Italia). Alcian blue kit was purchased from bio-Optica (Milan, Italy).

Collagen film formulation

COL films have been formulated using solvent casting technique. COL from bovine Achilles tendon (690 mg) was dissolved in acetic acid 0.5 M (315 ml). The solution was stirred for 1 h at 40°C. The suspension was homogenized with a mixer for 2 min at maximum speed, then blended and placed in five plates (60 ml/each), and left under the chemical hood for 36 h. The films were then detached by covering them with Milli-Q water and removing the edges with a spatula. Films' washing was done with the following steps: 15 min of washing with 20–40 ml of Milli-Q three times and then 15 min of washing with 10 ml of ethanol. Then, the films were deposited on polymeric support, left to dry for 30 min and then peeled off. COL films obtained were semitransparent, flexible and thin. The sample was called COL-CTRL.

Pristine collagen films functionalized with chondroitin sulfate

The COL film (COL-CTRL; 11 cm × 7 cm approximately, 105 mg, 0.036 mmol), obtained as previously described, was functionalized with CS (COL-CS; the protocol was adapted from [36]). The reaction was performed in a 12 cm × 8 cm plastic box. Briefly, CS (855 mg, 1.800 mmol) was dissolved in 40 ml citrate buffer solution pH 6.0 and COL film was immersed in the solution. After 30 min, $NaBH_3CN$ (56.5 mg, 0.900 mmol) was added and the reaction was left overnight. The day after, the film was sequentially washed three times for 15 min with saturated NaCl, Milli-Q water and ethanol. Then, the COL film was left to dry on polymeric support, and after 30 min peeled off.

Plasma treatment of collagen films

COL films have been formulated using solvent casting technique obtained as previously described (COL-CTRL) and then treated with NTP. The vacuum chamber was built in the Plasma Prometeo Center of the University of Milano-Bicocca. The system is composed of a cylindrical vacuum chamber with some openings, vacuum feed-throughs and sensors, a gas dispenser and pumping systems providing a low residual pressure of about 10^{-6} mbar. Plasma is produced by coupling to a capacitive antenna a radio frequency power generator. The antenna is composed of two parallel aluminum blades of diameter 19 cm with a distance maintained to 6 cm. The gas is injected into the chamber through the upper electrode, the surface of which is perforated with small evenly distributed holes. The antenna is connected to a 13.56 MHz radio frequency generator (Advanced Energy RFX-600, Assago, Italy) equipped with a matching network transmitting powers of the order of several tens of watts. After evacuation, the cylinder is filled with oxygen at the pressure of 0.45 mbar. During the plasma treatment, the system works with a rotary pump, equipped with a liquid nitrogen trap. In the present experiment power was set at 225 W and plasma treatment time was 2 min.

Plasma-treated COL-CS

The plasma-treated COL (COL-PLASMA) film (11 cm × 7 cm approximately, 105 mg, 0.036 mmol), obtained as previously described, was then functionalized with chondroitin sulphate (CS). Briefly, CS (855 mg, 1.800 mmol) was dissolved in 40 ml citrate buffer solution pH 6.0 and the COL film was immersed in the solution. After 30 min, $NaBH_3CN$ (56.5 mg, 0.900 mmol) was added and left overnight. The day after, the film was sequentially washed three times for 15 min with saturated NaCl, Milli-Q water and ethanol. Then, the COL film functionalized with CS (COL-CS) was left to dry on polymeric support, and after 30 min peeled off.

Characterization of plasma-treated & functionalized collagen films

FTIR spectroscopy

The FTIR spectra were recorded in attenuated total reflection mode using a PerkinElmer Spectrum 100 FTIR Spectrometer (MA, USA). The samples have been analyzed at different points of the material. The absorbances of the samples and backgrounds were measured using 60 scans each. The spectral absorption data were collected in the range between 4000 and 525 cm^{-1} at a spectral resolution of 0.5 cm^{-1}. Obtained spectra have been processed with OriginPro 2021 (64-bit) 9.8.0.200 (Academic) software.

Cell culture

U87 glioblastoma cell line (Sigma-Aldrich) were maintained in adhesion condition in T-75 tissue culture flasks. U87 cells were cultured in DMEM supplemented with 10% fetal bovine serum (FBS) serum, 100 units/ml penicillin and 100 mg/ml streptomycin at 37°C under a humidified atmosphere with 5% CO_2.

Biocompatibility

The viability of the cells on different COL films was evaluated using a LIVE/DEAD Viability/Cytotoxicity kit (Invitrogen®, Monza, Italy), following the manufacturer's instructions. The COL films (0.5 cm × 0.5 cm) were inserted into the wells of a 24-well with ethanol which was then subsequently removed and let evaporate under the hood until it was completely dry. The COL films were left for 30 min under UV-light for further sterilization. In total, 1 ml of the stock solutions was added to each sample. The cells were plated with a concentration of 1×10^4 cells/well in a 24-multiwell. After 40 min of incubation at 37°C the stained samples were washed with PBS before image acquisitions. Imaging analysis was performed with confocal microscopy, with Zeiss cell observer spinning disk microscope equipped with a sCmos (Milan, Italy) camera (Hamamatsu Orca Flesh V2.0, Arese, Italy) 10× phase-contrast objective. Cell viability was calculated using Fiji ImageJ software as:

$$\frac{\text{Live Cells}}{(\text{Live cells} + \text{Dead cells})} \times 100 = \%\ \text{Cell viability}$$

Cell adhesion rate after 1 day was calculated as a number of red stained cells/time using Fiji ImageJ software.

Immunofluorescence assay

Cell morphology on COL films was analyzed by actin/phalloidin-DAPI immunostaining. After removing the culture medium, each well was fixed with 1 ml of 4% paraformaldehyde for 1 h. After three washings of PBS for 15 min, 1 ml of permeabilization solution was added to each well and left for 1 h. The films were washed three times with PBS and 1 ml of blocking solution was added to each well and left overnight. Then films were washed three times again with PBS before the staining process. Blocking solution (50 ml) was prepared with 50 ml of PBS, 1.5 g of bovine serum albumin and 250 µl of Triton. Permeabilization solution (50 ml) was prepared with 5 g of sucrose, 2.5 ml of Triton, 300 mg of $MnCl_2$ and 46.5 ml of PBS. The samples were stained with 1 ml of a DAPI-phalloidin solution and left overnight. The samples were washed for, at least, 3 days with PBS 1× before imaging. Phalloidin stock solution was diluted at 1:100, while DAPI stock solution (5 mg/ml) was diluted at 1:1000. Cell imaging was performed by confocal microscopy. DAPI was used for staining the cell nuclei and phalloidin for the actin filaments. DAPI was excited at a wavelength of 405 nm (emitted wavelength: 420–520 nm). Phalloidin was excited at a wavelength of 540–545 nm (emitted wavelength: 570–573 nm).

Scanning electron microscopy analysis

Scanning electron microscopy (SEM) was employed to characterize the surface of the obtained COL films and scaffold. The morphology of the biomaterials was investigated by using a Field Emission Gun – Scanning Electron Microscope (FEG-SEM) Zeiss Gemini 500 (Milan, Italy) at 5 kV as voltage. Prior to examination, the samples were sputter-coated (10-nm gold layer) thanks to an Edwards S150B sputter coater for high-quality SEM applications (Crawley, West Sussex, UK). Qualitative analysis for surface elemental composition (chemical analysis) was performed by employing the energy dispersive x-ray spectroscopy (EDS) detector, with a working distance of 8.2 mm between the surface sample and the lens and 15 kV as voltage.

Alcian blue

For the Alcian blue quantification, the wells were rinsed three times with PBS 1× with 1% acetic acid and covered for 15 min after the application of enough Alcian blue solution. After repeating the rinsing action with PBS to optimize clarity, the plates were left to dry in hood and absorbance was measured at 630 nm. For the Alcian blue visualization, the protocol on the data sheet was followed. In short, the COL film was brought to distilled water, and 10 drops of reagent A were placed on the film. After 30 min of waiting time, the film was drained without washing. At this point, 10 additional drops of reagent B were applied and allowed to act for 10 min. After a round of washing in distilled water, 10 drops of reagent C were applied this time and allowed to act for 5 min only. After a second wash in distilled water, ascending alcohols were exploited to dehydrate the film. The latter was then cleared in xylene and mounted. At the end, the samples were observed at the confocal microscopy with a 10× objective. The degree of functionalization (DF) is calculated as:

$$DF = \frac{A\ (average\ sample)}{A\ (average\ control)} \times 100$$

For COL films functionalized with CS (COL-CS), COL-CTRL was used as control. For plasma-treated COL-CS (COL-PLASMA-CS), COL-PLASMA was used as control.

Statistical analysis

Results are presented as mean ± standard deviation and compared using one-way analysis of variance. Statistical significance was set at $p < 0.05$.

Results

In this work COL films were prepared by solvent casting technique (100–200 µm thick) and then functionalized with CS. In Figure 1A COL film (COL-CTRL) was functionalized with CS exploiting the 5% of lysine residues of the protein via reductive amination (COL-CS). In Figure 1B the surface of COL film was treated by plasma treatment (COL-PLASMA) and then functionalized with CS via reductive amination (COL-PLASMA-CS).

Effect of oxygen plasma upon surface topography

The surface topographies of all the samples were observed using SEM. In Figure 2 the untreated COL film

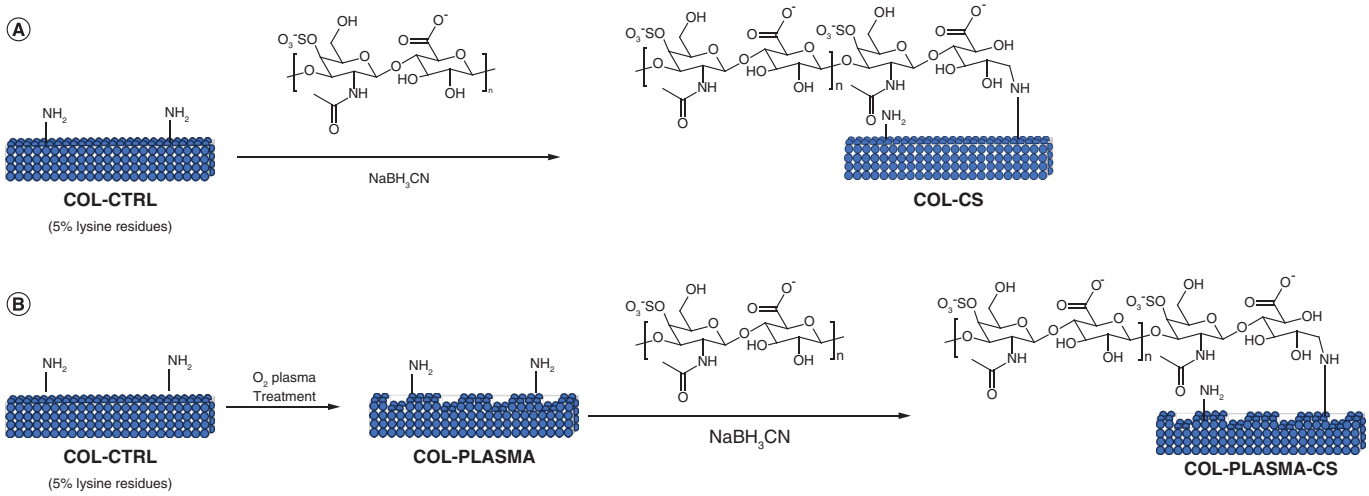

Figure 1. Functionalization approaches. (A) Reductive amination of collagen film (COL-CTRL) with chondroitin sulfate (COL-CS) and **(B)** nonthermal plasma treatment on collagen film (COL-PLASMA) and reductive amination with chondroitin sulfate (COL-PLASMA-CS). COL-CS: Collagen films functionalized with chondroitin sulfate; COL-CTRL: Control collagen film sample; COL-PLASMA: Plasma-treated collagen; COL-PLASMA-CS: Plasma-treated collagen functionalized with chondroitin sulfate.

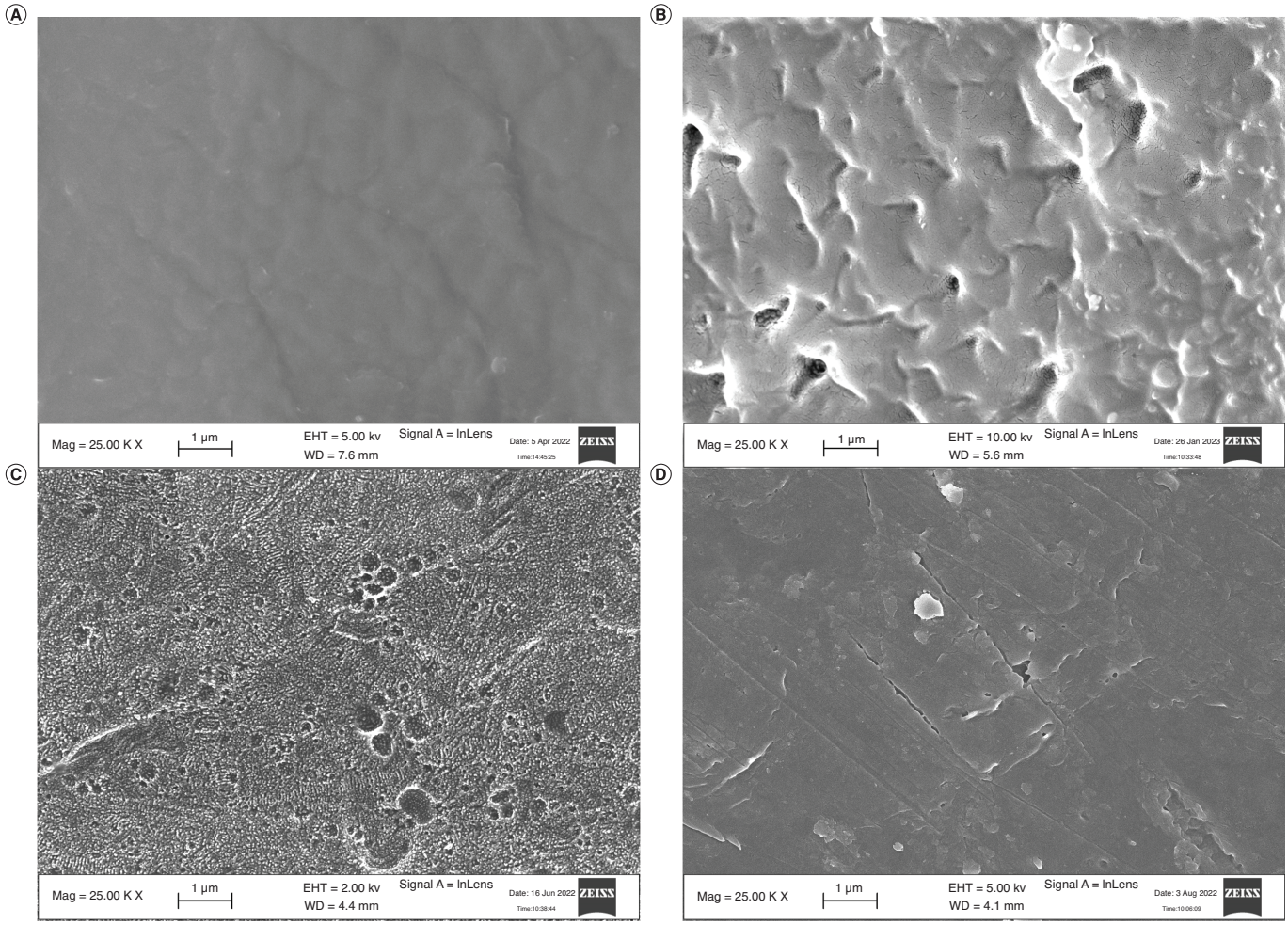

Figure 2. Scanning electron microscopy images. (A) Control collagen film sample, **(B)** collagen films functionalized with chondroitin sulfate, **(C)** plasma-treated collagen and **(D)** plasma-treated collagen functionalized with chondroitin sulfate.

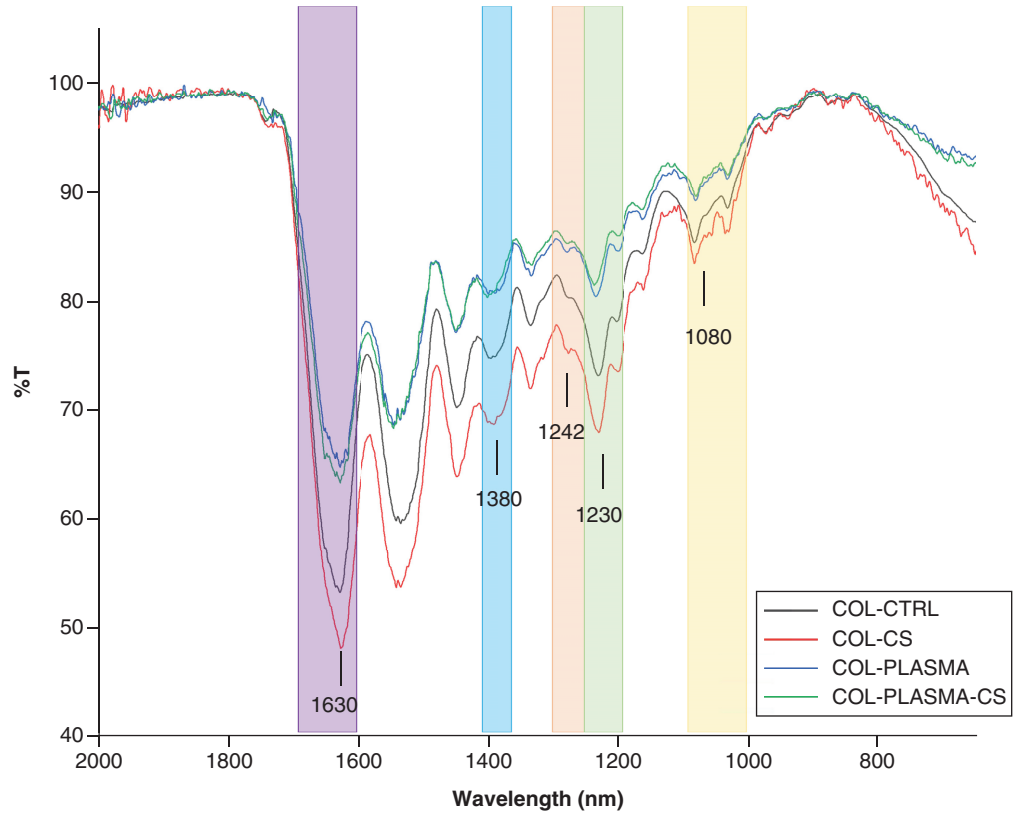

Figure 3. FTIR spectra of COL-PLASMA, COL-CTRL, COL-PLASMA-CS and COL-CS with a focus on 2000–750 cm^{-1} region.
COL-CS: Collagen films functionalized with chondroitin sulfate; COL-CTRL: Control collagen film sample; COL-PLASMA: Plasma-treated collagen; COL-PLASMA-CS: Plasma-treated collagen functionalized with chondroitin sulfate.
Note: '%T' in the y-axis refers to percentage of transmittance.

(COL-CTRL) presents an amorphous smooth surface without pores, while COL-CS presents an uneven coating distribution with a consequent increase in roughness. A marked difference is visible in the COL-PLASMA sample, where the film is characterized by pores resulting in higher roughness and etched features. Finally, in COL-PLASMA-CS the porous structures are missing in comparison to COL-PLASMA and instead present a smooth and homogeneous surface not observable in other samples. These features could be related to a differential interaction between the plasma-treated surface and the CS sulfated chains, resulting in more ordered and homogeneous structures on the surface of the film.

FTIR & Alcian blue evaluation

To monitor the effective functionalization with CS a FTIR analysis and an Alcian blue assay were performed. In Figure 3, COL film (COL-CTRL) was compared with the COL-CS, the COL-PLASMA and the COL-PLASMA-CS.

COL FTIR spectra exhibit absorptions in four characteristic spectral intervals: ν(C=O) absorption of amide I (1.630 cm^{-1}, purple), δ(CH_2) and δ(CH_3) absorptions (1380 cm^{-1}, in the light blue area), ν(C–N) and δ(N–H) absorptions of amide III (1230 cm^{-1}, in the green area), ν(C–O) and ν(C–O–C) absorptions of carbohydrate moieties (1080 cm^{-1}, marked in yellow) [37,38]. In the CS spectra, the region above 2000 cm^{-1} is dominated by the OH stretching vibration, the region around 1350 cm^{-1} is due to the sulfate, the band at 1242 cm^{-1} is due to S=O [39] (highlighted orange) and the peak at 850 cm^{-1} is due to the C–O–S vibration [40]. It is possible to observe that the peaks related to amide bonds do not change with the plasma treatment; in particular, peaks of amide I at 1630 cm^{-1} and amide III at 1454 cm^{-1} are comparable to untreated COL spectra. This result indicates the preservation of COL secondary structures after sample treatments [41].

The presence of CS has been evaluated and characterized also by Alcian blue (Figure 4) [42–45]. The lower

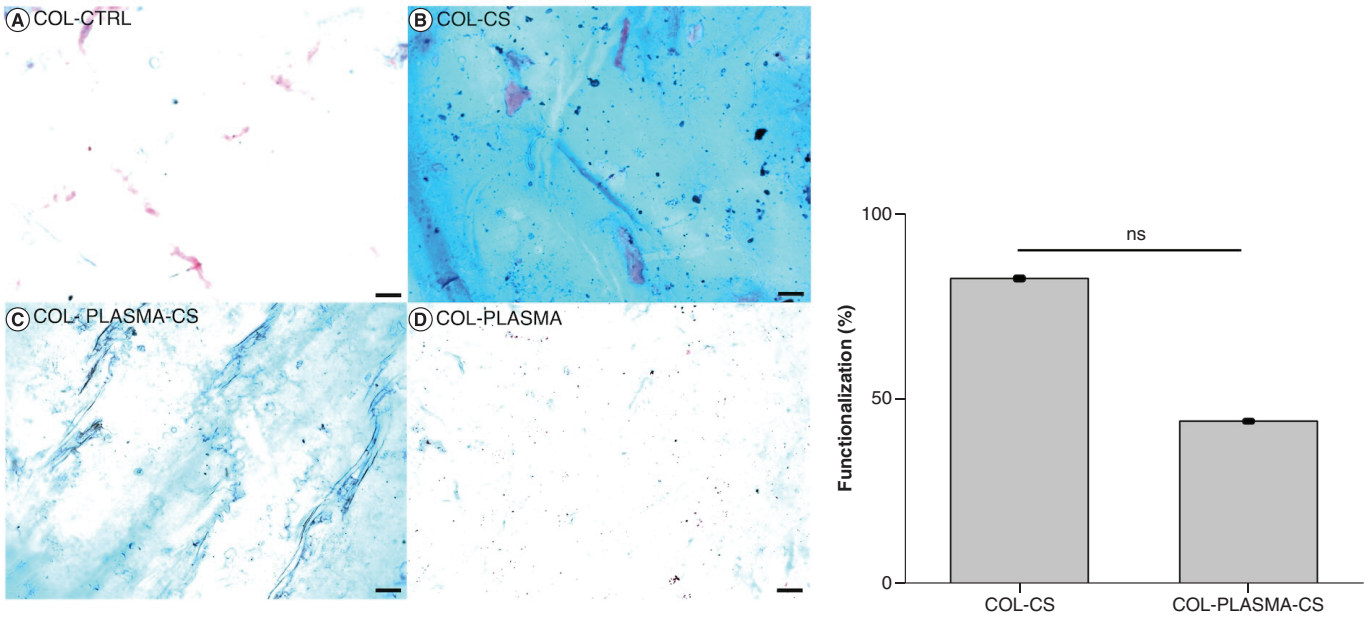

Figure 4. Alcian blue staining. (A) COL-CTRL, **(B)** COL-CS 82% ± 0.26 functionalized, **(C)** COL-PLASMA-CS 44% ± 0.14 functionalized and **(D)** COL-PLASMA (n = 4). Scale bar: 100 μm.
COL-CS: Collagen films functionalized with chondroitin sulfate; COL-CTRL: Control collagen film sample; COL-PLASMA: Plasma-treated collagen; COL-PLASMA-CS: Plasma-treated collagen functionalized with chondroitin sulfate; ns: Not significant.

functionalization degree in the COL-PLASMA-CS could be due to a better filming process of the CS coating rather than a poor functionalization, while the larger amount of functional groups in the COL-CS sample could outline the presence of larger clusters rather than thin-layer coating of CS.

Next, to evaluate the biocompatibility and the future application for tissue engineering application, U87-MG cells were cultured on the surface of COL-CS, COL-PLASMA and COL-PLASMA-CS, while COL-CTRL was used as a control. First, a live/dead assay at different time points was performed, confirming the biocompatibility of the functionalized biomaterials. From that, according to literature [46], the cell viability was then quantified (Figure 5B). Second, the cells were stained using phalloidin/DAPI to get information of their cytoskeleton architectures when exposed to the different treated COL films (Figure 5C). The outcomes of these analyses were the formation of more complex structures when the NTP and CS modifications were coupled (COL-PLASMA-CS), comparing to the single treatment COL-CS and COL-PLASMA. Moreover, these findings were also confirmed by the cell adhesion rate data (Figure 5D) obtaining by counting the red stained cells after 1 day (Figure 5D) [47].

Discussion

As evident from SEM images (Figure 2), visible changes in surface topography can be observed after oxygen treatment. Indeed, while the untreated COL film (COL-CTRL) presents an amorphous relatively smooth surface [19], the functionalization with CS forms a nonuniform coating on the glycosylated COL films (COL-CS) increasing the roughness of the film (similar to works reported in literature [48]). The presence of small pores and cluster structures seems to outline the not complete coating adhesion on the substrate. On the other hand, higher roughness, heterogeneous and porous structures occur in plasma-treated film (COL-PLASMA), as can be appreciated in Figure 2. In the COL-PLASMA sample, several structures at the microscale in the form of craters and at the nanoscale in the form of pillars appear. Structures are produced by competitive etching processes, in which energetic plasma species, such as oxygen atoms and charges, strike the surface promoting chemical reactions generating the desorption of volatile products in the gas phase, generating cavities on the substrate on the macroscale and pillars at the nanoscales. The multiscale complex structures behave homogeneously at the nanoscale, where pillars are in the order of nanometers (diameter of 30–50 nm), in the nanostructured surface [49]. This complex interface impacts the adhesion of the CS coating and the microscopic signatures on the cell growth.

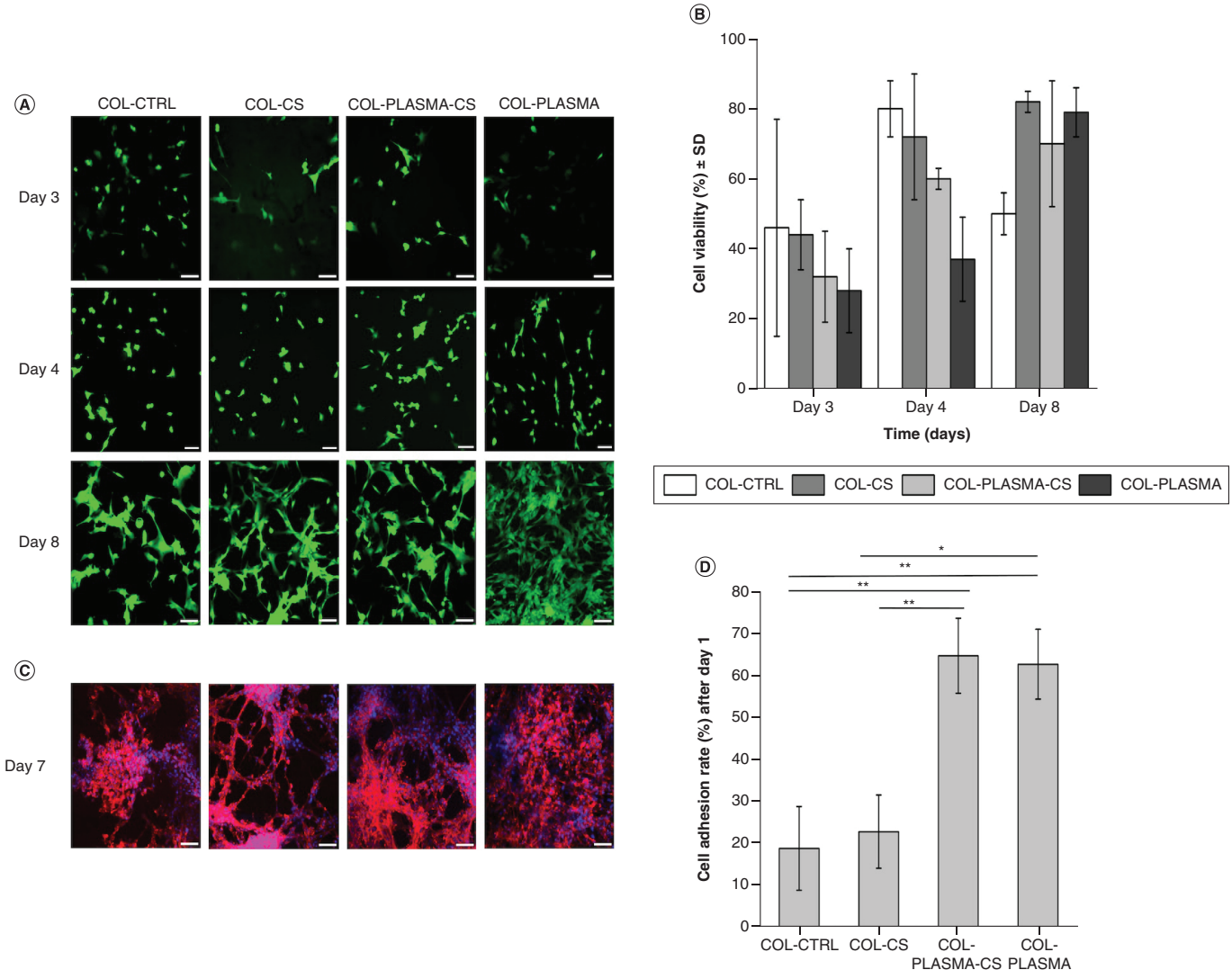

Figure 5. Cell viability and morphological analysis. (A) Live/dead staining of U87 cells on COL-CTRL, COL-PLASMA, COL-PLASMA-CS and COL-CS samples at different time points. **(B)** Cell viability % (± SD, n = 3) on COL-CTRL, COL-PLASMA, COL-PLASMA-CS and COL-CS after 3, 4 and 8 days. Cell viability was calculated as (number of green stained cells/number of total cells) × 100 using Fiji ImageJ software. **(C)** Immunofluorescence assay of U87 cells on COL-CTRL, COL-PLASMA, COL-PLASMA-CS and COL-CS samples. **(D)** Number of cells/cm^2 (± SD, n = 3) on day 1, day 8 and day 10 on the different functionalized collagen films. Number of cells per area was calculated as number of red stained cells/area using Fiji ImageJ software. **(E)** Cell adhesion rate (± SD, n = 3) after 1 day or 8 days on COL-CTRL, COL-CS, COL-PLASMA-CS and COL-PLASMA samples. Cell adhesion rate was calculated as a number of red stained cells/time using Fiji ImageJ software. Scale bar: 100 μm.
*$p < 0.005$; **$p < 0.01$; ***$p < 0.001$.
COL-CS: Collagen films functionalized with chondroitin sulfate; COL-CTRL: Control collagen film sample; COL-PLASMA: Plasma-treated collagen; COL-PLASMA-CS: Plasma-treated collagen functionalized with chondroitin sulfate; SD: Standard deviation.

While in COL-CS the CS coating was not homogeneous and did not adhere properly, on the contrary, the COL-PLASMA-CS was covered by a homogeneous and well-adherent CS layer, probably due to the interaction between the plasma-treated surface and the CS sulfated chains. The better adhesion of the CS coating on the surface will influence the cells' growth on the films.

Once confirmed the different surface topographies upon the COL films, the effective functionalization reaction was then confirmed by FTIR analysis and Alcian blue assay (Figures 3 & 4). Especially from the latter it is possible to notice that CS is not homogeneously distributed in the COL-PLASMA-CS compared with COL-CS. These findings were expected. Indeed, as previously shown from SEM images (Figure 2), the NTP treatment leads to the formation of pillars and structure that prevent the COL film being functionalized uniformly. These data were also

corroborated by the FTIR spectra from which the peaks corresponding to the sulfated groups are higher in intensity in the COL-CS compared with COL-PLASMA-CS and by the quantitative functionalization analysis (Figure 4).

Then, we were interested to verify if the different topographies and roughnesses of the COL films have an impact on cellular behavior and morphology. With this aim, we cultured U87-MG cells on the surface of all the different samples finding a comparable viability (average of 60% at day 8). For all the functionalized samples an increase of cell proliferation is notable compared with the untreated COL, especially on day 8, when the cells adhere to the substrate forming a monolayer (Figure 5B & C). According to literature [18,50], we could observe higher attachment and proliferation behavior relative to controls (Figure 5). Plasma surface treatment increases the adhesion properties of the surface to cells [51]. As can be seen in Figure 5D, the rate of cell adhesion in plasma-treated COL films was increased. More importantly, we can observe different morphology and structural cell organization on day 10 (Figure 5C). In brief, while the COL-CTRL and COL-PLASMA U87 cell lines appear to grow as monolayers, in the COL-CS they are exhibiting short filopodia-like structures with dendritic arborization [52–54], while in COL-PLASMA-CS the cells grow in a more branched arrangement and form a more complex architecture, starting clustering together. The topography of the ECM can significantly influence cell behavior. The topographical structure of the substrate has direct and evident effects on the ability of some cellular elements to orient themselves, to migrate and to reorganize the cytoskeleton. In the presence of different surface morphology the cell adheres to the substrate, significantly changing the structure of its own cytoskeleton [55]. Due to the dual stimulation the cells received, the cells on COL-PLASMA-CS grew faster and adhered better to the film. Cells grown on plasma-treated and functionalized films were stimulated both biochemically (due to CS) and morphologically (due to plasma). Both contributions are relevant, and this can be evidenced by the fact that the COL-PLASMA-CS sample has an 'enhanced' cell proliferation and morphology compared with single treatments.

Conclusion

The generation of bioactive material to mimic the ECM features and replicate the crosstalk between cells and the microenvironment requires control of the morphological and biochemical properties of the material's surface. We find that nonthermal plasma treatment is able to modify the surface of COL films providing scaffolds with improved properties for cell adhesion and proliferation once the signaling properties have been introduced by functionalization with CS. Indeed, our double-functionalized material showed higher cell adhesion and proliferation of U87 cells forming a tissue-like structure, thanks to the more homogeneous CS layer observed by SEM analysis in comparison to the control.

In conclusion, the NTP and the functionalization with CS results in an interesting methodology to finely tune and control both physical and biochemical properties for synthesizing ECM mimetics for biomedical applications.

Summary points

- The cell microenvironment contains a multitude of information capable of inducing different cellular modulation.
- The extracellular matrix is a crucial component in the development of functional tissues and its composition varies in a pathological state.
- To reproduce the cell–extracellular matrix crosstalk is essential to mimic both the physical and the biochemical signals.
- In this work we proposed a combined method to easily functionalize collagen surface films, also customizing their morphological properties.
- The physical and structural modification is obtained using oxygen nonthermal plasma treatment, while the biochemical stimulus is obtained through glyco-conjugation with chondroitin sulfate.
- Both the physical and the biochemical signals introduced led to a different surface morphology, analyzed by scanning electron microscopy.
- The double-functionalized material resulted in an increased adhesion, proliferation and morphological organization of U87 glioblastoma cells.
- The nonthermal plasma treatment and functionalization with chondroitin sulfate offer an intriguing strategy to fine-tune both physical and biochemical properties.
- Our finding suggests new promising strategies for the development of collagen-based biomaterials, which can be employed for advanced *in vitro* models.

Financial disclosure

This work was funded by the National Plan for NRRP Complementary Investments (PNC, established with the decree-law 6 May 2021, No. 59, converted by law No. 101 of 2021) in the call for the funding of research initiatives for technologies and innovative trajectories in the health and care sectors (Directorial Decree no. 931 of 06-06-2022) – project no. PNC0000003 – Advanced Technologies for Human-centred Medicine (ANTHEM). This work reflects only the authors' views and opinions: neither the Ministry for University and Research nor the European Commission can be considered responsible for them. The authors also received financial support from Ministero della Salute, Ricerca Finalizzata RF-2021-12371959 'Tackling immunomodulatory properties of stromal cells to improve therapeutic strategies in lung cancer' (30.4.2023-29.4.2026), and MUR PRIN 2022, 2022MY7AZT Dynamic multifunctional hydrogels for glioblastoma therapy (DINGO). The authors have no other relevant affiliations or financial involvement with any organization or entity with a financial interest in or financial conflict with the subject matter or materials discussed in the manuscript apart from those disclosed.

Competing interests disclosure

The authors have no competing interests or relevant affiliations with any organization or entity with the subject matter or materials discussed in the manuscript. This includes employment, consultancies, honoraria, stock ownership or options, expert testimony, grants or patents received or pending, or royalties.

Writing disclosure

No writing assistance was utilized in the production of this manuscript.

References

Papers of special note have been highlighted as: • of interest; •• of considerable interest

1. Nicolas J, Magli S, Rabbachin L, Sampaolesi S, Nicotra F, Russo L. 3D extracellular matrix mimics: fundamental concepts and role of materials chemistry to influence stem cell fate. *Biomacromolecules* 21(6), 1968–1994 (2020).

• **Provides an insightful overview of the main extracellular matrix components.**

2. Cadamuro F, Nicotra F, Russo L. 3D printed tissue models: from hydrogels to biomedical applications. *J. Control. Rel.* 354, 726–745 (2023).

3. Marino S, Menna G, Di Bonaventura R *et al.* The extracellular matrix in glioblastomas: a glance at its structural modifications in shaping the tumoral microenvironment – a systematic review. *Cancers* 15(6), 1879 (2023).

4. Cadamuro F, Marongiu L, Marino M *et al.* 3D bioprinted colorectal cancer models based on hyaluronic acid and signalling glycans. *Carbohydr. Polym.* 302, 120395 (2023).

• **Highlights the importance of glycosignatures at extracellular matrix level.**

5. Shoulders MD, Raines RT. Collagen structure and stability. *Annu. Rev. Biochem.* 78, 929–958 (2009).

6. Bose S, Li S, Mele E, Williams CJ, Silberschmidt VV. Stability and mechanical performance of collagen films under different environmental conditions. *Polym. Degrad. Stab.* 197, 109853 (2022).

7. Torres-Giner S, Gimeno-Alcañiz JV, Ocio MJ, Lagaron JM. Comparative performance of electrospun collagen nanofibers cross-linked by means of different methods. *ACS Appl. Mater. Interfaces* 1(1), 218–223 (2009).

8. Zhong S, Teo WE, Zhu X, Beuerman R, Ramakrishna S, Yung LYL. Formation of collagen – glycosaminoglycan blended nanofibrous scaffolds and their biological properties. *Biomacromolecules* 6(6), 2998–3004 (2005).

9. Prockop DJ, Kivirikko KI. Collagens: molecular biology, diseases, and potentials for therapy. *Annu. Rev. Biochem.* 64, 403–434 (1995).

10. Iida J, Meijne AML, Knutson JR, Furcht LT, McCarthy JB. Cell surface chondroitin sulfate proteoglycans in tumor cell adhesion, motility and invasion. *Semin. Cancer Biol.* 7(3), 155–162 (1996).

• **Highlights the role of chondroitin sulfate proteoglycans in modulating cellular adhesion.**

11. Djerbal L, Lortat-Jacob H, Kwok J. Chondroitin sulfates and their binding molecules in the central nervous system. *Glycoconj. J.* 34(3), 363–376 (2017).

12. Kanyo N, Kovacs KD, Saftics A *et al.* Glycocalyx regulates the strength and kinetics of cancer cell adhesion revealed by biophysical models based on high resolution label-free optical data. *Sci. Rep.* 10(1), 1–20 (2020).

13. Bandtlow CE, Zimmermann DR. Proteoglycans in the developing brain: new conceptual insights for old proteins. *Physiol. Rev.* 80(4), 1267–1290 (2000).

Taylor & Francis
Taylor & Francis Group

14. Horii-Hayashi N, Sasagawa T, Matsunaga W, Nishi M. Development and structural variety of the chondroitin sulfate proteoglycans-contained extracellular matrix in the mouse brain. *Neural Plast.* 2015, 256389 (2015).
15. Logun MT, Bisel NS, Tanasse EA *et al.* Glioma cell invasion is significantly enhanced in composite hydrogel matrices composed of chondroitin 4- and 4,6-sulfated glycosaminoglycans. *J. Mater. Chem. B* 4(36), 6052–6064 (2016).
16. Lin Y-C, Chu Y-H, Liao W-C *et al.* CHST11-modified chondroitin 4-sulfate as a potential therapeutic target for glioblastoma. *Am. J. Cancer Res.* 13(7), 2998 (2023).
17. Mellai M, Casalone C, Corona C *et al.* Chondroitin sulphate proteoglycans in the tumour microenvironment. *Adv. Exp. Med. Biol.* 1272, 73–92 (2020).
18. Pezeshki-Modaress M, Mirzadeh H, Zandi M *et al.* Gelatin/chondroitin sulfate nanofibrous scaffolds for stimulation of wound healing: *in-vitro* and *in-vivo* study. *J. Biomed. Mater. Res. A* 105(7), 2020–2034 (2017).
19. Cadamuro F, Ferrario M, Akbari R, Antonini C, Nicotra F, Russo L. Tyrosine glucosylation of collagen films exploiting horseradish peroxidase (HRP). *Carbohydr. Res.* 533, 108938 (2023).
20. Karumbaiah L, Enam SF, Brown AC *et al.* Chondroitin sulfate glycosaminoglycan hydrogels create endogenous niches for neural stem cells. *Bioconjug. Chem.* 26(12), 2336–2349 (2015).
21. Latchoumane CFV, Chopra P, Sun L *et al.* Synthetic heparan sulfate hydrogels regulate neurotrophic factor signaling and neuronal network activity. *ACS Appl. Mater. Interfaces* 14(25), 28476–28488 (2022).
22. Schuurmans CCL, Brouwer AJ, Jong JAW, Boons GJPH, Hennink WE, Vermonden T. Hydrolytic (in)stability of methacrylate esters in covalently cross-linked hydrogels based on chondroitin sulfate and hyaluronic acid methacrylate. *ACS Omega* 6(40), 26302–26310 (2021).
23. Ao Y, Tang W, Tan H, Li J, Wang F, Yang L. Hydrogel composed of type II collagen, chondroitin sulfate and hyaluronic acid for cartilage tissue engineering. *Biomed. Mater. Eng.* 33(6), 515–523 (2022).
24. Maarof M, Nadzir MM, Mun LS *et al.* Hybrid collagen hydrogel/chondroitin-4-sulphate fortified with dermal fibroblast conditioned medium for skin therapeutic application. *Polymers (Basel)* 13(4), 508 (2021).
25. Zhang L, Li K, Xiao W *et al.* Preparation of collagen-chondroitin sulfate-hyaluronic acid hybrid hydrogel scaffolds and cell compatibility *in vitro*. *Carbohydr. Polym.* 84(1), 118–125 (2011).
26. Costa RR, Caballero D, Soares da Costa D *et al.* Microfluidic-assisted interfacial complexation of extracellular matrix components to mimic the properties of neural tissues. *Adv. Mater. Technol.* 8(19), 2300983 (2023).
27. Booth JP, Mozetič M, Nikiforov A, Oehr C. Foundations of plasma surface functionalization of polymers for industrial and biological applications. *Plasma Sources Sci. Technol.* 31(10), 103001 (2022).
28. Zanini S, Zoia L, Della Pergola R, Riccardi C. Pulsed plasma-polymerized 2-isopropenyl-2-oxazoline coatings: chemical characterization and reactivity studies. *Surf. Coatings Technol.* 334, 173–181 (2018).
29. Dell'Orto EC, Vaccaro A, Riccardi C. Morphological and chemical analysis of PP film treated by dielectric barrier discharge. *J. Phys Conf. Ser.* 550(1), 012032 (2014).
30. Dell'Orto EC, Caldirola S, Sassella A, Morandi V, Riccardi C. Growth and properties of nanostructured titanium dioxide deposited by supersonic plasma jet deposition. *Appl. Surf. Sci.* 425, 407–415 (2017).
31. Russo L, Zanini S, Riccardi C, Nicotra F, Cipolla L. Diazo transfer for azido-functional surfaces. *Mater. Today* 14(4), 164–169 (2011).
32. Yoshida S, Hagiwara K, Hasebe T, Hotta A. Surface modification of polymers by plasma treatments for the enhancement of biocompatibility and controlled drug release. *Surf. Coatings Technol.* 233, 99–107 (2013).
33. Piferi C, Bazaka K, D'Aversa DL *et al.* Hydrophilicity and hydrophobicity control of plasma-treated surfaces via fractal parameters. *Adv. Mater. Interfaces* 8(19), (2021).
34. Choi HS, Kim Young-Sun Y, Zhang Y, Tang S, Myung SW, Shin BC. Plasma-induced graft co-polymerization of acrylic acid onto the polyurethane surface. *Surf. Coatings Technol.* 182(1), 55–64 (2004).
35. Sharma R, Kuche K, Thakor P *et al.* Chondroitin sulfate: emerging biomaterial for biopharmaceutical purpose and tissue engineering. *Carbohydr. Polym.* 286, 119305 (2022).
36. Raspanti M, Caravà E, Sgambato A, Natalello A, Russo L, Cipolla L. The collaggrecan: synthesis and visualization of an artificial proteoglycan. *Int. J. Biol. Macromol.* 86, 65–70 (2016).
37. Belbachir K, Noreen R, Gouspillou G, Petibois C. Collagen types analysis and differentiation by FTIR spectroscopy. *Anal. Bioanal. Chem.* 395(3), 829–837 (2009).
38. Riaz T, Zeeshan R, Zarif F *et al.* FTIR analysis of natural and synthetic collagen. *Appl. Spectrosc. Rev.* 53(9), 703–746 (2018).
39. Akhshabi S, Biazar E, Singh V, Heidari Keshel S, Nagaraja G. The effect of glutaraldehyde cross-linker on structural and biocompatibility properties of collagen-chondroitin sulfate electrospun mat. *Mater. Technol.* 33(4), 253–261 (2018).

•• **Helped the authors regarding the FTIR spectra interpretation.**

40. Alberto-Silva C, Blini F, Malheiros M, Querobino SM. Fourier-transformed infrared spectroscopy, physicochemical and biochemical properties of chondroitin sulfate and glucosamine as supporting information on quality control of raw materials. *Future J. Pharm. Sci.* 6(1), 1–9 (2020).

41. Samouillan V, Merbahi N, Yousfi M *et al.* Effect of low-temperature plasma jet on thermal stability and physical structure of type I collagen. *IEEE Trans. Plasma Sci.* 40(6 part 2), 1688–1695 (2012).

42. Hao J-X, Wan Q-Q, Mu Z *et al.* A seminal perspective on the role of chondroitin sulfate in biomineralization. *Carbohydr. Polym.* 310, 120738 (2023).

43. Karlsson M, Björnsson S. Quantitation of proteoglycans in biological fluids using Alcian blue. *Methods Mol. Biol.* 171, 159–173 (2001).

44. Frazier SB, Roodhouse KA, Hourcade DE, Zhang L. The quantification of glycosaminoglycans: a comparison of HPLC, carbazole, and Alcian blue methods. *Open Glycosci.* 1(1), 31 (2008).

●● **Helped the authors to set up the protocol for Alcian blue quantification.**

45. Andersson E, Tykesson E, Lohmander LS *et al.* Quantification of chondroitin sulfate, hyaluronic acid and N-glycans in synovial fluid – a technical performance study. *Osteoarthr. Cartil. Open.* 5(3), 100380 (2023).

46. Spaepen P, De Boodt S, Aerts JM, Sloten JV. Digital image processing of live/dead staining. *Methods Mol. Biol.* 740, 209–230 (2011).

47. Carnaggio JA, Smith JA, Penno MB. Phalloidin-based fluorimetric quantitation of cells on plates and polycarbonate membranes. *Methods Cell Sci.* 17(4), 263–270 (1995).

48. Fajardo AR, Lopes LC, Caleare AO *et al.* Silver sulfadiazine loaded chitosan/chondroitin sulfate films for a potential wound dressing application. *Mater. Sci. Eng. C* 33(2), 588–595 (2013).

49. Chen R, Curran J, Pu F, Zhuola Z, Bayon Y, Hunt JA. *In vitro* response of human peripheral blood mononuclear cells (PBMC) to collagen films treated with cold plasma. *Polymers (Basel)* 9(7), 254 (2017).

50. Jin J, Tilve S, Huang Z, Zhou L, Geller HM, Yu P. Effect of chondroitin sulfate proteoglycans on neuronal cell adhesion, spreading and neurite growth in culture. *Neural Regen. Res.* 13(2), 289–297 (2018).

51. Moll P, Pfusterschmied G, Schneider M *et al.* Biocompatible a-SiC:H-based bistable MEMS membranes with piezoelectric switching capability in fluids. *J. Microelectromech. Syst.* 31(3), 372–383 (2022).

52. Mencio CP, Hussein RK, Panpan Y, Geller HM. The role of chondroitin sulfate proteoglycans in nervous system development. *J. Histochem. Cytochem.* 69(1), 61–80 (2021).

53. Salazar K, Espinoza F, Cerda-Gallardo G *et al.* SVCT2 overexpression and ascorbic acid uptake increase cortical neuron differentiation, which is dependent on vitamin c recycling between neurons and astrocytes. *Antioxidants (Basel)* 10(9), 1413 (2021).

54. Dansie LE, Ethell IM. Casting a net on dendritic spines: the extracellular matrix and its receptors. *Dev. Neurobiol.* 71(11), 956–981 (2011).

55. Curtis ASG, Casey B, Gallagher JO, Pasqui D, Wood MA, Wilkinson CDW. Substratum nanotopography and the adhesion of biological cells. Are symmetry or regularity of nanotopography important? *Biophys. Chem.* 94(3), 275–283 (2001).